



**Electrochemical synthesis of small-sized red fluorescent
graphene quantum dots as a bioimaging platform**

Journal:	<i>ChemComm</i>
Manuscript ID:	CC-COM-11-2014-009332.R1
Article Type:	Communication
Date Submitted by the Author:	17-Dec-2014
Complete List of Authors:	Tan, Xiaoyun; Beijing Normal University, Chemistry Li, Yunchao; Beijing Normal University, Dept. of Chemistry Li, Xiaohong; Chemistry, Zhou, Shixin; Peking University Health Science Center, Department of Cell Biology Fan, Louzhen; Beijing Normal University, Chemistry Yang, Shihe; The Hong Kong University of Science and Technology, Department of Chemistry

Cite this: DOI: 10.1039/c0xx00000x

www.rsc.org/xxxxxx

ARTICLE TYPE

Electrochemical synthesis of small-sized red fluorescent graphene quantum dots as a bioimaging platform

Xiaoyun Tan,^a Yunchao Li,^a Xiaohong Li,^a Shixin Zhou,^b Louzhen Fan,^{*a} and Shihe Yang^{*c}

Received (in XXX, XXX) Xth XXXXXXXXX 20XX, Accepted Xth XXXXXXXXX 20XX

DOI: 10.1039/b000000x

We report water-soluble, 3 nm uniform-sized graphene quantum dots (GQDs) with red emission prepared by electrochemical exfoliation of graphite in K₂S₂O₈ solution. Such GQDs show a great potential as biological labels for cellular imaging.

Graphene quantum dots (GQDs) have attracted much recent attention due to their ultrafine dimensions, tunable surface functionalities and economical synthetic routes. The stable photoluminescence (PL) and low toxicity make them outstanding as an alternative to organic dyes and inorganic quantum dots (QDs) in biological applications.¹ On the other hand, due to the auto-fluorescence and light scattering background of biological specimens in the short-wavelength region, fluorescent materials of choice are expected to emit in the long-wavelength region in order to provide a deeper light penetration into the specimens, resulting in a higher imaging contrast. To date, most of the reported GQDs emit the blue to green fluorescence, which usually exhibits excitation wavelength dependence². The most effective ways of tuning the optical properties of GQDs are to develop fluorescent labelled GQDs by covalent modification with organic dyes or to prepare large size GQDs in order to keep a high conjugation extent. However, the complicated preparation limits their application and the resulting GQDs are too big to enter cells. We have reported water-soluble GQDs with strong yellow PL as a robust biological label for stem cells by electrochemical method.^{3,4} Herein, we report the facile electrochemical exfoliation of graphite in K₂S₂O₈ solution for the synthesis of uniform small-sized red fluorescent GQDs (RF-GQDs) without any chemical modification, which has been used for cellular imaging.

The RF-GQDs was prepared by electrolysis of graphite in 0.01 M K₂S₂O₈ aqueous solution at a potential of +5.0 V (see the supporting information for details). Figure 1a and b display transmission electron microscope (TEM) images of RF-GQDs, exhibiting a size of about 3 nm in diameter. The atomic force

microscopy (AFM) image (Figure 1c, d) demonstrates the topographic morphology of GQDs, and confirms that all of the GQDs have a thickness <1 nm, corresponding to 1–3 graphene layers.⁵ As shown in Figure 1e, corresponding to the X-ray diffraction (XRD) pattern of the pristine graphite of one prominent peak centered at around 26° for its (002) planes, RF-GQDs exhibit a weak broad peak, which is attributed to the thinness and disordered stacking of GQDs.⁶ The Raman spectrum of RF-GQDs (Figure 1f) shows the characteristic G band at 1601 cm⁻¹ and D band at 1350 cm⁻¹ with an intensity ratio I_D/I_G of ca. 1.0. The ratio is lower than what was commonly reported GQDs (1.23) prepared by similar methods,³ indicating fewer defects on RF-GQDs (Figure S1, 2).

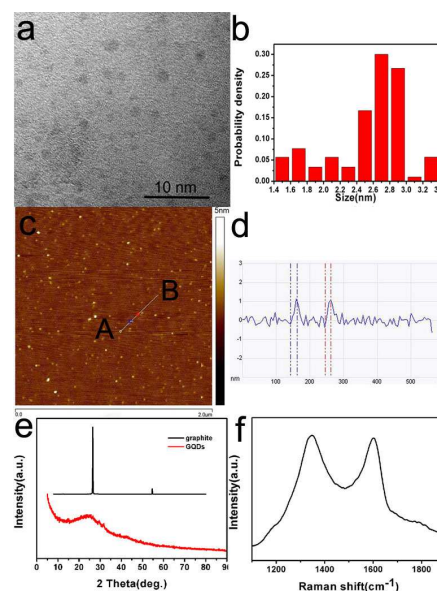


Figure 1 (a) TEM images and (b) size distribution of RF-GQDs. (c) AFM image and (d) height profile along the line from A to B (inset) of RF-GQDs deposited on freshly cleaved mica substrates. (e) XRD patterns of the pristine graphite and RF-GQDs. (f) Raman spectrum of RF-GQDs.

The most distinctive feature of RF-GQDs which sets them apart from other previously reported GQDs is the specific PL they emit. From the UV-vis spectrum of RF-GQDs aqueous solution (Figure 2a), the typical absorption peak at 227 nm could be assigned to the π - π^* transition of graphitic sp² domains.⁷ As shown in Figure 2b, on excitation at the wavelength of 500 nm, the PL spectrum

^a Department of Chemistry, Beijing Normal University, Beijing, 100875, China. E-mail: lzfan@bnu.edu.cn

^b Department of Cell Biology, School of Basic Medicine, Peking University Health Science Center, Beijing, 100191, China

^c Department of Chemistry, The Hong Kong University of Science and Technology, Clear Water Bay, Kowloon, Hong Kong, China

† Electronic Supplementary Information (ESI) available: See DOI: 10.1039/b000000x/

shows the strongest peak at 610 nm. When excited by light with wavelengths from 340 to 520 nm, the intensity of the PL increased to the maximum then decreased, but the fluorescent emission peak remained unshifted, indicating that the PL origin of RF-GQDs is markedly dissimilar to that of the common excitation wavelength dependent PL of graphene oxide quantum dots and other carbon quantum dots, which was commonly attributed to the size effect of carbon quantum dots (Figure S3, 4).

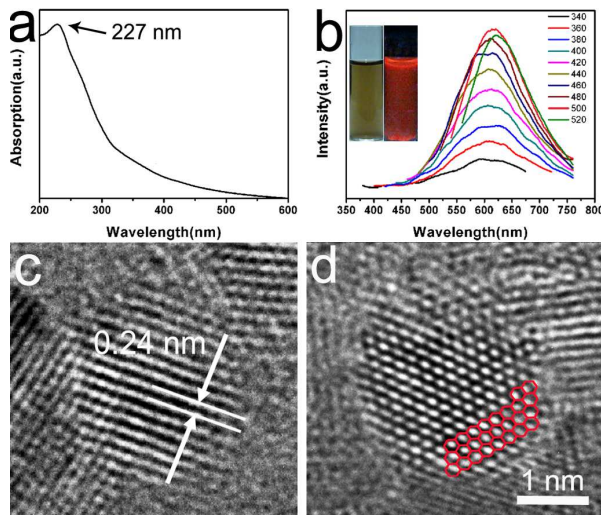


Figure 2 UV-vis absorption (a) and PL (b) spectra of RF-GQDs aqueous solution. The inset of (b) is the photograph of the RF-GQDs solution under day light and 365 nm illumination. HRTEM image with measured lattice spacing (c) and sp^2 domains (d) of RF-GQDs.

Efforts were made to characterize the origin of the red luminescence of RF-GQDs with very uniform small size of 3 nm and without any chemical modification. The high-resolution transmission electron microscopy (HRTEM) image (Figure 2c) clearly shows the lattice spacing of RF-GQDs is 0.24 nm which is corresponding to the (1120) lattice fringes of graphene, indicating that most of the dots are actually separate graphenes. Furthermore, as indicated in red colour in Figure 2d, the carbon hexagon structures for one dot have been readily observed. They are arranged orderly and the visible well-crystallized carbon areas almost occupy the whole dot. The blurred boundary may attribute to amorphous carbon areas caused by the introduction of oxygenic groups. It is noteworthy that no obvious defect can be seen in the whole images and this structure is reproducible observed in most of the RF-GQDs (see Figure S5), which implies that RF-GQDs are consist of intact sp^2 clusters. It has been reported previously that most of prepared GQDs were considered to be consist of small sp^2 clusters isolated within the sp^3 carbon matrix.⁸ The energy gap between the π and π^* states generally depends on the size of sp^2 clusters or conjugation length⁹. A sp^2 cluster of more than 40 aromatic rings has energy gap of around 2 eV which can convert into about 600 nm PL.¹⁰ Larger sp^2 clusters have lower energy gap and may emit at red light region. In this view, we deduce that large sp^2 clusters of RF-GQDs are likely to be responsible for their red PL. To be the best of our knowledge, this is the first report about the direct observation of “molecular” sp^2 domains with a diameter of ca. 3 nm which has a red emission.

Two facets should be related to the efficient direct exfoliation

of graphite into small-sized and red-emission GQDs without degrading their sp^2 bonded carbon network structure. First, the electrochemical oxidative cleavage efficiently exfoliates the graphite into graphene sheets.^{3, 4, 11} Second, the supporting electrolyte, $K_2S_2O_8$ is crucial for generating the specific GQDs, which was verified by control experiments. When the supporting electrolyte was changed to the other strong oxidants such as K_2FeO_4 with the even higher standard electrode potential ($E^\ominus = 2.20$ V) than $K_2S_2O_8$ ($E^\ominus = 2.01$ V) under otherwise the same experimental conditions, no any light could be observed for the as-synthesized solution upon irradiation with UV lamp. It suggests that the strong oxidizability of $K_2S_2O_8$ is not in relation to the generation of RF-GQDs. However, when sulphate (Na_2SO_4) was selected as supporting electrolyte, the similar red but very weak PL behaviour could be observed (Figure S6). As reported, there are $S_2O_8^{2-}$ ions to be produced by a large anodic voltage discharging of SO_4^{2-} .¹² And the strong oxidizing $SO_4^{\cdot-}$ radicals are to be generated by electrochemical reaction of $S_2O_8^{2-}$.¹³ We believe that the very active $SO_4^{\cdot-}$ radicals may serve as electrochemical “scissors” to sharply cut the graphene sheets into small intact sp^2 structures by oxidizing the C–C bonds. It is clearly that $K_2S_2O_8$ as a particular supporting electrolyte which can produce active radical is the key factor for RF-GQDs.

Taken together, it is evident that under the given electrochemical reaction conditions, the 3 nm GQDs with intact sp^2 domain without defects can be obtained. Taking a step further, the PL properties can be tuned by controlling the size of sp^2 domains. 30% H_2O_2 aqueous solution, which was reported to be capable to break C-C bond, extend topological defects and result in the formation of smaller sp^2 fragments,¹⁴ was then added into 5 mg mL⁻¹ RF-GQDs solution and heated at 70°C for different time. The GQDs solution emitted yellow fluorescence at 550 nm after three hours. Six hours later, the emission turned to green fluorescence at about 500 nm. After twelve hours, the GQDs solution emitted blue fluorescence at 420 nm. As shown in Figure 3, the emission peak has a blueshift with progressive oxidation treatment by H_2O_2 , demonstrating that the size of sp^2 domains of GQDs determines the local energy gap and therefore the wavelength of the emitted fluorescence.

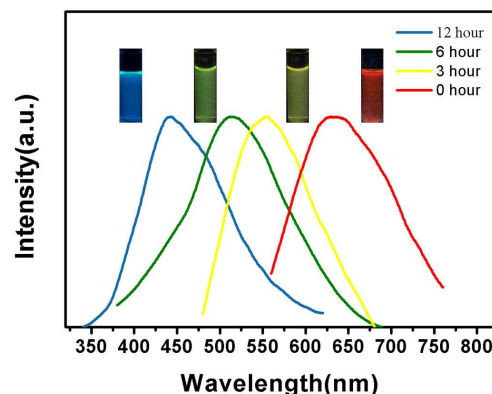


Figure 3 Normalized PL spectra of progressively oxidized RF-GQDs at different time under 360 nm laser excitation. The insets show photographs of the corresponding GQDs solutions.

The water soluble, small-sized, and red PL RF-GQD without any surface modifications impart them outstanding applications

of biological labels for cellular imaging. As shown in Figure 4a and b, RF-GQDs are able to label both the cell membrane and the cytoplasm of HeLa cells with red emission under 488 nm excitation in a significant fashion, which demonstrates that the translocation of RF-GQDs from outside the cell membrane into the cytoplasm (Figure S7). Moreover, with several runs of repeated excitation, no intensity change of fluorescence could be observed, indicating high photostability of RF-GQDs in the cells. Figure 4c shows the viability of HeLa cells after incubation with RF-GQDs for 24 h by three parallel MTT (tetrazolium salt reduction) experiments. No significant loss of cell viability was observed with the concentration of incubated RF-GQDs 1000 $\mu\text{g mL}^{-1}$. These results show great potential of RF-GQDs for biomedical applications, indicating that they can be used for direct and efficient cell labelling.

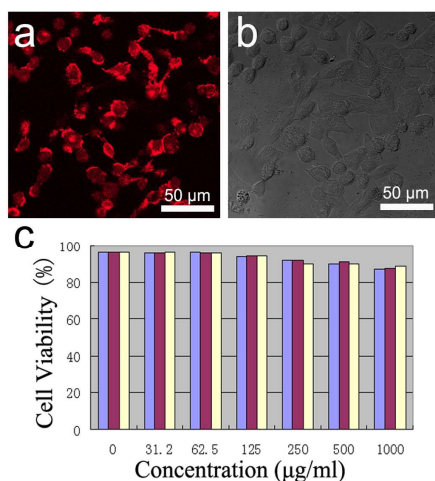


Figure 4 (a) Confocal fluorescence microscopy images of HeLa cells with RF-GQDs incorporated at the excitation wavelength of 488 nm and corresponding image under bright field (b). (c) Cell viability for the HeLa cells as a function of the added RF-GQDs concentration.

In summary, we have successfully prepared water-soluble, 3 nm uniform-sized red emission RF-GQDs without any chemical modification by electrochemical exfoliation of graphite in $\text{K}_2\text{S}_2\text{O}_8$ solution. RF-GQDs are demonstrated to be isolated sp^2 domains with a diameter of ca. 3 nm generated by the very active $\text{SO}_4^{\cdot-}$ radicals produced from $\text{S}_2\text{O}_8^{2-}$ as electrochemical “scissors” to sharply cut the graphene sheets into small intact sp^2 structures. Such GQDs have shown excellent optical property in biomedical applications with good photostability and little cytotoxicity. Such GQDs are expected to have potential in various biomedical applications. Detailed follow-up work is underway in our laboratory and will be reported in due course.

This work is supported by NSFC (21073018), the Major Research Plan of NSFC (21233003), the Fundamental Research Funds for the Central Universities, Key Laboratory of Theoretical and Computational Photochemistry and RGC of Hong Kong (GRF No. 606511).

Notes and references

1 (a) S. N. Baker, G. A. Baker, *Angew. Chem. Int. Ed.* 2010, **49**, 6726-6744; (b) J. Shen, Y. Zhu, C. Chen, X. Yang, C. Li, *Chem. Commun.* 2011, **47**, 2580; (c) K. Habiba, V. I. Makarov, J. Avalos, M. J. F. Guinel, B. R. Weiner, G. Morell, *Carbon* 2013, **64**, 341; (d) M. Xie, Y. Su, X. Lu, Y. Zhang, Z. Yang, Y. Zhang, *Mater. Lett.* 2013, **93**,

161; (e) Y. Dong, H. Pang, S. Ren, C. Chen, Y. Chi, T. Yu, *Carbon* 2013, **64**, 245; (f) J. Shen, Y. Zhu, X. Yang, Li, C., *Chem. Commun.* 2012, **48**, 3686.

2 (a) W. Chen, F. Li, C. Wu, T. Guo, *Appl. Phys. Lett.* 2014, **104** (b) P. Russo, A. Hu, G. Compagnini, W. W. Duley, N. Y. Zhou, *Nanoscale* 2014, **6**, 2381; (c) Y. Feng, J. Zhao, X. Yan, F. Tang, Q. Xue, *Carbon* 2014, **66**, 334; (d) Q. Xu, Q. Zhou, Z. Hua, Q. Xue, C. Zhang, X. Wang, D. Pan, M. Xiao, *ACS Nano* 2013, **7**, 10654; (e) Y. Li, Y. Zhao, H. Cheng, Y. Hu, G. Shi, L. Dai, L. Qu, *J. Am. Chem. Soc.* 2011, **134**, 15; (f) V. Gupta, N. Chaudhary, R. Srivastava, G. D. Sharma, R. Bhardwaj, S. Chand, *J. Am. Chem. Soc.* 2011, **133**, 9960; Zhang, M.; Bai, L.; Shang, W.; Xie, W.; Ma, H.; Fu, Y.; Fang, D.; Sun, H.; (g) Z. Qian, J. Ma, X. Shan, L. Shao, J. Zhou, J. Chen, H. Feng, *RSC Adv.* 2013, **3**, 14571; (h) Z. Qian, J. Zhou, J. Chen, C. Wang, C. Chen, H. Feng, *J. Mater. Chem.* 2011, **21**, 17635.

3 M. Zhang, L. Bai, W. Shang, W. Xie, H. Ma, D. Fang, H. Sun, L. Fan, L.; Han, M.; Liu, C.; Yang, S., *J. Mater. Chem.* 2012, **22**, 7461.

4 Z. Fan, Y. Li, X. Li, L. Fan, S. Zhou, D. Fang, S. Yang, *Carbon* 2014, **70**, 149.

5 X. Li, X. Wang, L. Zhang, S. Lee, H. Dai, *Science* 2008, **319**, 1229.

6 Y. Li, Y. Hu, Y. Zhao, G. Shi, L. Deng, Y. Hou, L. Qu, *Adv. Mater.* 2011, **23**, 776.

7 D. Pan, J. Zhang, Z. Li, C. Wu, X. Yan, M. Wu, *Chem. Commun.* 2010, **46**, 3681.

8 (a) C. Mattevi, G. Eda, S. Agnoli, S. Miller, K. A. Mkhoyan, O. Celik, D. Mastrogiovanni, G. Granozzi, E. Garfunkel, M. Chhowalla, *Adv. Funct. Mater.* 2009, **19**, 2577; (b) M. Ishigami, J. H. Chen, W. G. Cullen, M. S. Fuhrer, E. D. Williams, *Nano Lett.* 2007, **7**, 1643; (c) K. N. Kudin, B. Ozbas, H. C. Schniepp, R. K. Prud'homme, I. A. Aksay, R. Car, *Nano Lett.* 2007, **8**, 36; (d) J. I. Paredes, S. Villar-Rodil, P. Solís-Fernández, A. Martínez-Alonso, J. M. D. Tascón, *Langmuir* 2009, **25**, 5957; (e) C. Gómez-Navarro, J. C. Meyer, R. S. Sundaram, A. Chuvilin, S. Kurasch, M. Burghard, K. Kern, U. Kaiser, *Nano Lett.* 2010, **10**, 1144; (f) I. J. ung, D. A. Field, N. J. Clark, Y. Zhu, D. Yang, R. D. Piner, S. Stankovich, D. A. Dikin, H. Geisler, C. A. Ventrice, R. S. Ruoff, *J. Phys. Chem. C* 2009, **113**, 18480; (g) N. R. Wilson, P. A. Pandey, R. Beanland, R. J. Young, I. A. Kinloch, L. Gong, Z. Liu, K. Suenaga, J. P. Rourke, S. J. York, J. Sloan, *ACS Nano* 2009, **3**, 2547.

9 C. W. Chen, J. Robertson, *J. Non-Cryst. Solids* 1998, 227–230, **Part 1**, 602.

10 G. Eda, Y. Y. Lin, C. Mattevi, H. Yamaguchi, H. A. Chen, I. S. Chen, C. W. Chen, M. Chhowalla, *Adv. Mater.* 2010, **22**, 505.

11 (a) S. Li, Y. Li, J. Cao, J. Zhu, L. Fan, X. Li, *Anal. Chem.* 2014, **86**, 10201; (b) T. Li, Y. Li, L. Lu, H. Tao, L. Fan, *Acta. Chimica. Sinica.* 2014, **72**, 227.

12 J. Balej, M. Kaderavek, *Collect. Czech. Chem. Commun.* 1979, **44**, 1510

13 L. Li, J. Ji, R. Fei, C. Z. Wang, Q. Lu, J. R. Zhang, L. P. Jiang, J. J. Zhu, *Adv. Funct. Mater.* 2012, **22**, 2971.

14 F. Jiang, D. Chen, R. Li, Y. Wang, G. Zhang, S. Li, J. Zhen, N. Huang, Y. Gu, C. Wang, C. Shu, *Nanoscale* 2013, **5**, 1137.